Proton Uptake by Dormant Bacterial Spores

S. Kazakov

*Department of Chemistry and Physical Sciences, Pace University
861 Bedford Road, Pleasantville, NY, USA, skazakov@pace.edu

ABSTRACT

Recently, the type of proton ionizable groups, their exact number, and equilibrium proton binding constant have been determined for dormant *Bacillus subtilis* spores [1]. Kinetics of proton exchange between spores and surrounding aqueous solution supposes to be complicated mostly because of two coupled factors: a presumably high negative net charge and a multi-layered structure of the spore matrix. Indeed, in this work, we show by time-resolved micro-potentiometry [2] that proton uptake kinetics was a multi-step process involving a number of successively ~10-fold slower steps of proton penetration into the bulk and their binding to the ionizable groups within different layers of a spore structure. The important conclusion derived from the time constants systematically presented for the spore structural layers is that the effective diffusion coefficient for hydrogen ions within the spore core is significantly lower than the one within coats and cortex. Assuming the case of coupled proton diffusion and binding within the spore layers, the concentrations of ionizable groups in the spore compartments are estimated to be comparable with the gigantic spore proton capacity obtained from the data on proton equilibrium binding. In the practical point of view, regulation of the spore internal pH may be the way of its metabolic dormancy control, since the internal pH may be a contributing factor to enzymatic activity within the dormant spore.

Keywords: *Bacillus* spores, natural ionic reservoirs, spore proton capacity, kinetics of pH-equilibration.

1 INTRODUCTION

By now, it is well established (see, for example, refs. 1-11 in [1]) that charged groups attached to polymer chains play an essential role in the ionic sensitivity of polymer networks. We have already suggested [3] that dormant spores of bacteria are naturally occurred microcapsules which could behave like ionic hydrogels capable of uptaking and releasing ions. A hydrogel-like structure and its ionic sensitivity may be attributed to all integuments of spore. The analogy of the spore cortex with ionic hydrogel is straightforward. The spore cortex is a peptidoglycan polymer located between the spore inner and outer membranes. The cortex possesses a negative net charge. The low degree of cross-linking [4] supposes that the spore cortex is able to change volume in response to ionic changes as a result of balancing the electrostatic interactions of charged peptidoglycan chains and their network elasticity. It has been proposed earlier [5] that biopolymers in the spore core are cross-linked to form an ion-sensitive gel-like structure. The spore coats also have the protein-borne structures resembling biopolymer networks [6].

One can easily imagine that the access of molecules to the spore interior may be restricted by their size, hydrophobicity, and binding affinity whereas their mobility within distinct spore structural compartments may be different. In this work, we show that the transitional kinetics of approaching the ionic equilibrium in the spores' suspension reflects those differences. Following the concept of the simultaneous proton diffusion and binding to ionizable groups, we are able to realize that the effect of proton binding to ionizable groups is in slowing the diffusion process. Herein, the extent to which the diffusion coefficients of protons are lowered inside a spore depends on the concentration of ionizable groups [n] and apparent binding constant K, as well as the initial concentration of protons at the very beginning of proton uptake. The proton capacity of *B. subtilis* spores found from equilibrium data [1] appeared to be high, [n] ~ 35 M. In this work, we decided to estimate the concentration of ionizable groups [n] from the kinetic data (the times for diffusion of protons through different layers of the spore) and the sizes of spore compartments determined by using *B. subtilis* spore electron micrograph [6].

2 EXPERIMENTAL SECTION

2.1 Spore Treatments

The *Bacillus subtilis* strain (1A700) used in this study was available from the culture collection of Department of Microbiology at University of Alabama (Birmingham, AL). For spore purification, the method of lysozyme treatment and salt-detergent washes was used. The purified spores were washed three times and finally stored in deionized water at 4°C. The stock suspension of *Bacillus subtilis* spores was tested to have the initial concentration of 1.18×10^9 spores/mL and pH~8.8. The concentration of spores was determined spectroscopically by measuring absorbance at 600 nm using a Lambda 2 UV-VIS spectrometer (Perkin Elmer, GmbH.) and microscopically using a Digital Optical Microscope DC3-163-PH (Microscope World, CA). All concentration measurements were carried out at room temperature (~25°C).

2.2 pH Measurements

The apparatus for pH real-time measurements provided the injection of acid or base into the inner volume without perturbations of the electrode. A MI-415 micro-combination electrode (Microelectrodes Inc., Bedford, NH) was used for pH measurements. Milli-Q water with initial pH ~ 5.85 was used for the reference titration. The pH was adjusted with 0.1 M HCl. The needed volume of water or spore suspension was poured into the cuvette. pH was equilibrated upon stirring. After 30-100 sec of recording the signals, acid or spore suspension was injected into the cuvette to have the total volume of 1 mL. The measurements were carried out with a sample time of 0.1 sec. it was found that when a certain amount of spores is injected into the aqueous solution, the accumulation of protons by spores begins immediately after their injection, so that the relative changes in pH are limited only by the rate of electronic circuitry which seems to be significantly less than the sample time used (0.1 sec). All measurements were carried out at room temperature. A Vernier Logger Pro (version 2.3) software was used for data acquisition, analysis and storage in real time.

2.3 Average Size of Spores

Dynamic Light Scattering (DLS) measurements of the *Bacillus subtilis* spore sizes were carried out on a "PhotoCor Complex" Photon Correlation Spectrometer (PhotoCor Instruments Inc., MD) utilizing a 10 mW He-Ne laser as a light source. The measurements were done at the constant scattering angle of 90°. Suspensions of spores were diluted to the concentration of 2.3×10^7 sp/mL and filtered into a cylindrical glass cuvette (∅10 mm) using a 2 μm Millipore Millex filter. The cumulant analysis was successfully used to give the average size and polydispersity of spores. In addition, particle size distribution analysis with an automatic or visually assisted choice of a regularization level was carried out using the DynaLS software (ver. 2, Alango Ltd., Israel). The reported spore size is the result of averaging those 25-30 measurements.

3 RESULTS AND DISCUSSIONS

3.1 pH-kinetics of *Bacillus subtilus* Spores

Figures 1 shows plots of the pH_{out}–kinetics for spore suspensions of two different concentrations immerged into aqueous solutions of different pH. It can be seen that the process of pH equilibration is a multi-step one and requires more than 1 hour to get the final value of pH external to spores. A fast increase in pH_{out} during the first second after spores' injection can be assigned to an intensive penetration of hydrogen ions into the pre-surface layer of the spores. For the samples with a relatively low initial pH_{out}, (pH_{ini} ~ 2–3.6, depending on the number of spores), the kinks with positive derivatives are observed on the pH_{out}–kinetic curves to indicate that an efflux of protons may appear in one-two seconds after spore injections. There are several interplaying processes which slow down the kinetics of proton consumption by spores in the interval from singles to thousands of seconds. The balancing of these steps may decrease, increase, or even stop proton consumption depending on the concentration of protons and concentration of spores. Our assumption is that the kinetics of proton uptake is the result of coupling diffusion and binding processes. If so, more precisely, the shape of pH_{out}–kinetic curve depends not only on the proton concentration gradient, but also on [n], the total concentration of ionizable groups inside each layer of the spore structure.

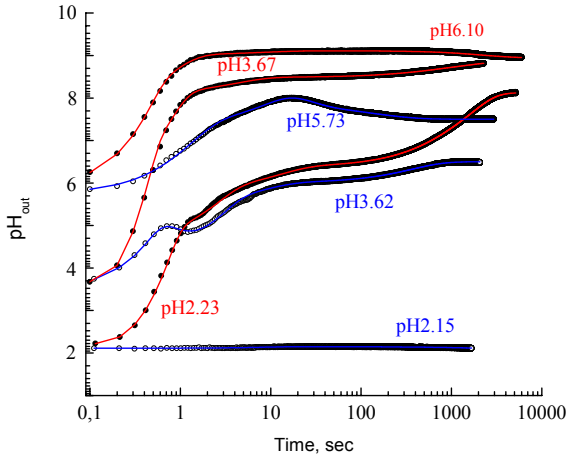

Figure 1: The time courses of external pH_{out} measured in the *B. subtilis* spore suspensions: prepared by injection of 0.5 mL of the stock suspension (1.18×10^9 sp/mL) into 0.5 mL of aqueous HCl solutions with the pH indicated for each red curve and prepared by injection of 20 μL of the stock suspension into 980 μL of aqueous HCl solutions with the pH indicated for each blu curve. Points are the experimental data, curves are the fitting curves.

The kinetics of proton penetration into the interior of spores can be represented as a set of *n* monomolecular reversible reactions

$$X_0 \underset{k_{-1}}{\overset{k_1}{\rightleftarrows}} X_1 \underset{k_{-2}}{\overset{k_2}{\rightleftarrows}} \ldots \underset{k_{-n}}{\overset{k_n}{\rightleftarrows}} X_n \,, \qquad (1)$$

where $X_0 = [H^+]_{out} = 10^{-pH_{out}}$ is the external concentration of free protons, X_i is the concentration of protons bound in a distinct layer of the spore structure, k_i and k_{-i} are the rate constants for the forward and reversible binding reactions, respectively.

It is known from chemical kinetics [8] that the solution of the system of *n* linear differential equations of the first

order for this scheme is the superposition of *n* exponential functions

$$X_i = X_i^{eq} + \sum_{j=1}^{n} A_{ji} e^{-t/\tau_j} \qquad (2)$$

where X_i^{eq} is the equilibrium concentration of protons, A_{ji} are the factors which contain the rate constants and depend on the initial conditions, τ_j are the characteristic times of the processes and are the functions of all rate constants k_i, k_{-i}. It is essential to note that the number of exponentially decaying functions corresponds to the number of reversible processes involved into equilibration, but n is not known *a priori*. The minimum number of exponential functions was used to fit each curve in Figure 1. Table 1 represents the characteristic times derived from the fitting of those curves and their possible interpretation as kinetically distinct steps describing $[H^+]$-equilibration.

Table 1: Distribution of the diffusion times (in seconds) through the spore structural layers.

$C_{sp} = 5.9\times10^8$ sp/mL			$C_{sp} = 2.3\times10^7$ sp/mL			**Spore compartments**
pH6.1	**pH3.67**	**pH2.23**	**pH5.73**	**pH3.62**	**pH2.15**	
0.09						*Unstirred layer:* ***~2nm***
0.4	0.05 0.2	0.11	0.3	0.25		*Outer coat:* ***~69nm***
8	3	1	0.65	1		*Inner+outer coats:* ***~119nm***
803	322	8	8.9	5.6	4	*Coats+cortex:* ***~251nm***
2007	1164	252 693	175	250	3089	*Coats+cortex+core:* ***~631nm***

3.2 *B. subtilis* Spore Compartments

To interpret the fast and slow time constants represented in Table 1, we estimated the thickness of outer coat, inner coat, cortex and core for *B. subtilis* spore using its electron micrograph from [6]. The contours of the spore compartments are shown in Figure 2.

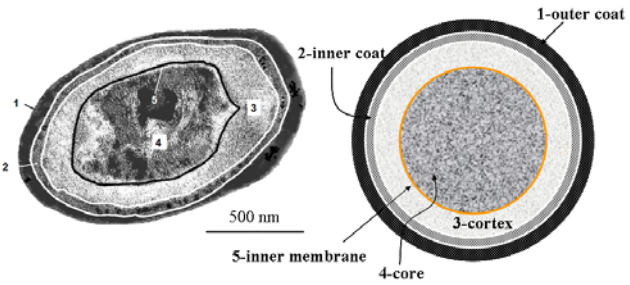

Figure 2: Contours of *B. subtilis* spore compartments adopted from the electron micrograph in [6] (left) and equivalent multilayered structure (right).

The areas edged by those contours have been calculated and the average radius of each area has been estimated, as the radius of equivalent sphere. The total average radius of the spore was estimated to be ~631 nm. The uncertainties were not less than ±10 nm in those calculations, so that the value of the total average spore radius looks very close to the value observed in our DLS measurements. The average hydrodynamic radius of the non-heat activated *B. subtilis* spores in the suspension containing 2.3×10^7 sp/mL was measured to be of (629±5) nm at room temperature and pH 7.5.

3.3 "Film" Controlled and "Particle" Controlled Diffusion

Two types of ion exchange are existed in a multi-layered structure like a spore (Figure 3). One is limited by diffusivity of ions within each layer ("film" diffusion), and other is limited by diffusivity of ions within the core ("particle" diffusion) [7]. The time constant for the "particle" controlled diffusion is

$$\tau = \frac{r^2}{\pi^2 D_{eff}}, \qquad (3)$$

where r is the radius of a particle and D_{eff} is the effective diffusion coefficient of protons within the particle. Eq. (3) was used for calculations of the effective diffusion coefficient within the spore core or the whole spore if the respective radii are known.

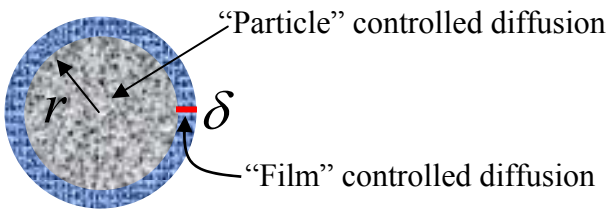

Figure 3: Two types of ion exchange in a multi-layered structure like a spore.

The time constant for the "film" controlled diffusion in the case of a single type of counter-ions (spores are diluted in pure water or in HCl solution and, no other counter-ions except hydrogen ions are present) is:

$$\tau = \frac{r\delta}{3D_{eff}}, \qquad (4)$$

where r is the radius of a spherical particle on which the film is deposited, δ is the thickness of the film, and D_{eff} is the effective diffusion coefficient of protons in the film. Eq. (4) was used for calculations of the effective diffusion coefficient within spore layers (coats and cortex).

Our data in Table 1 show that at low initial pH, the diffusion times for the fluxes of protons across the distance including the core radius were hundreds times slower than those for the spore coats and cortex (cf. 693/8 ≈ 87, 3089/4 ≈ 772). The corresponding ratios of effective diffusion coefficients were estimated as the ratio of D_{eff}^{core} for the core (particle controlled diffusion by Eq. 3) and

NSTI-Nanotech 2008, www.nsti.org, ISBN 978-1-4200-8504-4 Vol. 2

$D_{eff}^{coats+cortex}$ for the coats/cortex layer (film controlled diffusion by Eq. 4)

$$D_{eff}^{core} / D_{eff}^{coats+cortex} \approx 0.3 r \tau_{coats+cortex} / \delta \tau_{core},$$

to be $5.2 \cdot 10^{-3}$ and $5.9 \cdot 10^{-4}$, respectively.

3.4 Coupled Proton Diffusion and Binding within Spore's Compartments

In the course of modeling of diffusion and binding coupling in the spore matrix, it was assumed that (i) the process of ion binding to the matrix is rapid in comparison to diffusion, i.e. the local equilibrium always exists between free and bound ions; (ii) the diffusion coefficient of an ion in water D_{ion} is constant and does not vary with concentration and time; (iii) the changes in volume are negligible, and (iii) the concentration of protons at the diffusing front $[H^+]_{front}$ does not significantly change. Under these assumptions, the effective diffusion coefficient in the case of binding is given by [9]

$$D_{eff} = \frac{D_{ion}}{1 + \frac{[n]K}{(1 + K[H^+]_{front})^2}}, \qquad (5)$$

where [n] and K are the average concentration of binding sites in a spore compartment and the apparent binding constant, respectively. The expression (5) shows that the effect of proton binding to ionizable groups is in slowing the diffusion process. The degree to which the diffusion coefficients of protons are lowered inside a spore depends on balancing the concentration of binding sites and the initial gradient of protons. The distribution of binding site concentrations [n] along the spore structural layers was estimated by combining equations (3) – (5) for the model represented in Figure 3. Results are systemized in Table 2. Herein, diffusion coefficient for protons in water, $D_{ion} = 9.38 \times 10^9$ nm^2/s [10] and equilibrium binding constant $K = 5 \times 10^4$ M^{-1} [1], whereas diffusion times, τ, layer thicknesses, δ, and radii of a central core, r, are taken from Table 1.

Table 2: Estimated concentrations of binding sites inside the spore layered structure.

Spore compartments	Thickness of layer (δ), nm	Radius of central core (r), nm	[n], M
Unstirred layer	~2	~629	**~4**
Outer coat	~69	~562	**~4-6**
Inner+outer coats	~119	~512	**~6-9**
Coats+cortex	~251	~380	**~20-30**
Coats+cortex+core:		~631	**n/a***

*n/a – Eq.(5) is not applicable.

4 CONCLUSIONS

In this paper we have introduced a method of time-resolved micro-potentiometry for probing the kinetics of proton uptake by dormant *Bacillus subtilis* spores. It was shown that the plurality of steps comprising the uptake of protons may be attributed to the multi-layered coats-cortex-inner membrane-core structure of the spores. Particularly, based on the diffusion time analysis, it was found that the effective diffusion coefficient for hydrogen ions within the spore core can be up to 3 orders of magnitude lower than that within the coats and cortex.

The estimated concentrations of binding sites inside the spore layered structure appeared to be comparable with the average proton capacity of spores found from the equilibrium proton binding data [1]. Together with the known facts of (i) the low level of water (25-55% of the mass of the hydrated dormant spore core) in the spore cytoplasm or core, (ii) the bound state of water in the spore core, (iii) the high level of dipicolinic acid (DPA, ~5-15% of the mass of the hydrated spore core), (iv) the immobility of a soluble protein in dormant spores, and (v) the inner membrane lipids immobility, the high concentration of ionizable groups found in this work supposes that the spore cytoplasm is a particular state of biological matter characterized by a high density of charge within the nanosized matrix of the spore core.

This work was financially supported in part by Pace University (Dyson College of Art and Sciences, Summer Research Grant, Scholarly Research Fund, and Forensic Science Program). Acknowledgement is made to the Donors of the American Chemical Society/Petroleum Research Fund for partial support of this research (PRF grant # 44161-GB5).

REFERENCES

[1] S. Kazakov et al., J. Phys. Chem. B, 112, 2233, 2008.
[2] S. Kazakov et al., J. Phys. Chem. B, 110, 15107, 2006.
[3] S. Kazakov et al., NSTI-Nanotech 2007, 2, 692, 2007.
[4] D.L. Popham, P. Setlow, J.Bacteriol., 175, 2767, 1993.
[5] S.H. Black, P. Gerhardt, J. Bacterial. 83, 967, 1962.
[6] A. Driks, Microbiol. Mol. Biol. Rev. 63, 1, 1999.
[7] P.E. Marszalek et al., Biophys. J., 73, 1169, 1997.
[8] Cantor and Schimmel, "Biophysical Chemistry, Part III. The Behavior of Biological Macromolecules", Freeman & Co, 1980.
[9] P.E. Grimshaw, et al. J. Chem. Phys., 93, 4462, 1990.
[10] G.M. Eichenbaum, et al. Macromolecules, 31, 5084, 1998.